Viscoelastic interfacial modes in a wetting layer

D. Bonn and G. H. Wegdam
Van der Waals-Zeeman Laboratory, Nieuwe Achtergracht 127, 1018 WS Amsterdam, The Netherlands
(Received 19 October 1992)

Brillouin scattering from an evanescent wave enables us to study the dynamic structure factor $S(k,\omega)$ of fluids within 1 μm of a solid wall. Two interfacial fluid modes are found in a demixed binary-fluid system where a wetting layer of the heavy phase intrudes between the lighter phase and the solid wall. Surprisingly, the propagation velocity of one of these modes differs significantly from that of the corresponding bulk mode. A hydrodynamic calculation reveals that the alteration of the velocity cannot be explained in terms of continuity of the bulk transport properties over the interface. We propose that the shift in the propagation velocity is due to the viscoelastic character of the fluid-fluid interface.

PACS number(s): 68.45.−v, 68.10.−m

INTRODUCTION

The existence of hydrodynamic surface modes and their dispersion relations has been studied extensively in recent years [1–3]. The reason for this interest is twofold. First, the dispersion relation of these interface waves contains information on the transport of energy or momentum across interfaces [4]. This could be of interest for areas as diverse as the study of surface chemical reactions [4], fluid mechanics [5], and seismology [6]. Second, measurement of these interfacial waves might provide more insight into the microscopic structure of the transition region between two bulk fluid phases [7–9]. In most phenomenological treatments, the surface is described as a step profile in the density rather than a separate phase in which the order parameter changes continuously from one phase to another. In the latter case, several groups have shown that the surface transport properties are not necessarily the same as those of the bulk fluid. The notion of, for instance, a *surface viscosity* [10] that is different from the bulk one seems to have been generally accepted. As for the interface waves, it has been proposed [7] that the response of the surface is viscous at low frequencies, elastic at high frequencies, and viscoelastic in the intermediate regime.

For molecular liquids, most of the experimental studies so far have focused on the low-frequency regime where capillary waves are the dominant contribution to the structure factor [11,12]. At somewhat higher frequencies, measurements at the interface between a solid and a liquid have shown that an interfacial fluid mode can exist with a propagation velocity equal to that of the bulk sound mode [13]. Also, Dil and Brody [14] have found that an interfacial wave propagates along a liquid-vapor interface with a velocity equal to the longitudinal sound velocity in the liquid.

In this paper we present light-scattering measurements of the dynamic structure factor $S(k,\omega)$ in the cyclohexane-methanol binary-liquid system, where a thin wetting layer ($\cong$300 Å) of the methanol-rich phase intrudes between the cyclohexane-rich phase and the walls of a quartz container [15]. This remarkable phenomenon has been studied extensively in recent years [16,17], but so far no attention has been paid to the equilibrium fluctuations in such thin layers. We show that, when the reciprocal of the wave vector k in the scattering experiment is comparable to the layer thickness d, $kd \cong 1$, two interfacial fluid modes exist. One of these two modes has a propagation velocity *higher* than the bulk sound velocity in either of the two phases. A hydrodynamic calculation, where the interfacial stresses are calculated using the bulk transport coefficients, cannot successfully account for this finding. It is therefore proposed that the disagreement between theory and experiment is due to the viscoelasticity of the interface. This enables us to make an estimate of the magnitude of the elasticity modulus.

EXPERIMENT

At the critical concentration, the wetting transition takes place [17] at $T=294$ K. The experiments were performed at 298 K. The measuring cell is shown in Fig. 1(a). Half of the cell consists of a quartz semicylinder

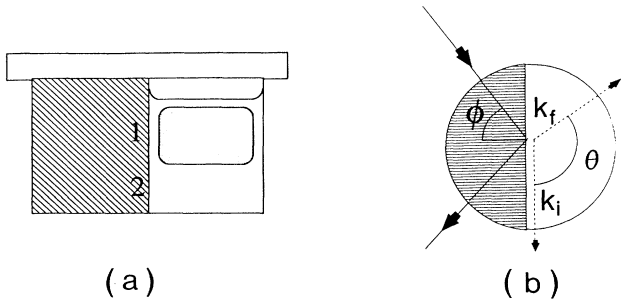

FIG. 1. (a) Schematic side view of the measuring cell. The left-hand side is the quartz semicylinder; the right-hand side is filled with the binary-fluid system. The measurements are performed at two different heights in the cell: 2 denotes the interface of the quartz with the methanol-rich phase; in 1 there is a wetting layer present in the scattering volume. (b) Top view of the measuring cell; the angle of incidence ϕ determines the penetration depth of the evanescent wave. The scattering angle is denoted as θ.

(shaded area); the other half can be filled with the binary-fluid system. The methanol-rich phase is the most dense phase and intrudes between the cyclohexane-rich phase and the quartz wall. The cyclohexane and methanol are filtered through a 0.22-μm Millipore filter. The sample had a critical temperature of 50.4 °C, suggesting the presence of 0.2 wt % water impurity [17]. The quartz is polished to small scale deviations from flatness less than $\lambda/20$, cleaned with a chromic acid solution, rinsed many times with water, and then dried.

The experimental setup is shown in Fig. 2. An Ar-ion laser ($\lambda=514.5$ nm) is focused in the center of the cell at the quartz-liquid interface. The angle of incidence of the laser beam, ϕ, is slightly larger than the critical angle of the total internal reflection ϕ_c. This is depicted in Fig. 1(b), where the scattering geometry is shown schematically. The beam is totally reflected at the quartz-liquid interface, generating an evanescent wave (EVW) in the liquid, which propagates along the boundary in the plane of incidence. The field of the EVW decays exponentially from the interface into the bulk with a penetration depth depending on the difference between the angle of incidence ϕ_i and the critical angle of total internal reflection ϕ_c [18]:

$$\xi_{\mathrm{EVW}}=(\lambda/2\pi n_{\mathrm{quartz}})(\sin^2\phi_i-\sin^2\phi_c)^{-1/2}\ . \qquad (1)$$

The penetration depth can therefore be varied experimentally, and has a typical value $\xi_{\mathrm{EVW}}=1.34$ μm for $\phi=\phi_c+0.2°$. This field with a real wave vector k_i parallel to the interface and an imaginary component equal to the inverse penetration depth acts as a source for scattering. The scattered light with wave vector k_f is collected and analyzed by a triple-pass Fabry-Pérot interferometer with a free spectral range $\nu_{\mathrm{FSR}}=2.68\times10^{10}\ \mathrm{s}^{-1}$.

The measurements are performed at two different heights in the measuring cell, denoted as 1 and 2 in Fig. 1(a). In the latter case, one measures the dynamic structure factor at a solid-liquid interface. In the former case, there is a wetting layer present in the scattering volume. In this geometry, the effective index of refraction can be estimated from the critical angle of total internal reflection [19]. This shows the index of refraction to be close to that of the cyclohexane-rich phase, $n_{\mathrm{eff}}=1.405$, while $n_{\mathrm{c\ rich}}=1.42$ and $n_{\mathrm{m\ rich}}=1.35$; $n_{\mathrm{quartz}}=1.46$. Having found the effective index of refraction in the liquid half-space, we can relate the absolute value and the tangential component of the wave vector $\bar{k}$ to the scattering angle θ as $k=2k_f\sin(\frac{1}{2}\theta)$ and $k_{\parallel}=2k_f\sin^2(\frac{1}{2}\theta)$, respectively, where $k_f=2\pi n_{\mathrm{eff}}/\lambda$. In this way, one obtains the dynamic structure factor $S(k,\omega)$ with $\omega=\omega_f-\omega_i$ for a fixed value of $\Delta\bar{k}=\bar{k}_f-\bar{k}_i$ [20].

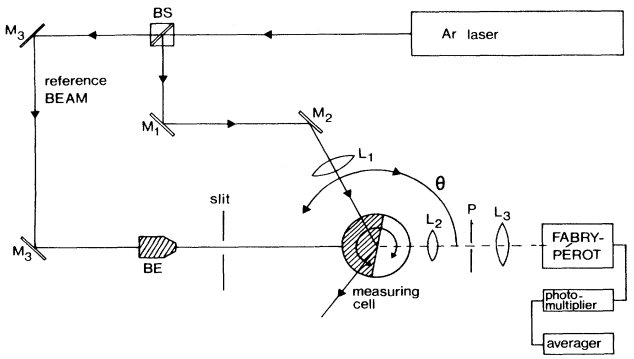

FIG. 2. Schematic view of the experimental setup. The angle of incidence and the scattering angle can be varied independently. BS = beam splitter, M = mirror, BE = beam expander, L = lens, P = pin hole.

RESULTS

A typical measurement of the structure factor with a wetting layer present in the scattering volume is shown in Fig. 3, where we depict two spectra with approximately the same scattering wave vector but with a different penetration depth of the evanescent wave. As is evident from the figure, we observe several propagating modes, which can be identified by their wave-vector dependence and propagation velocities. By plotting the frequencies as a function of the wave vector, we are able to identify the longitudinal sound mode of the solid (peaks *D* and *E*) and a bulk liquid sound mode (peak *C*) with a sound velocity that equals that of the cyclohexane-rich phase. These can

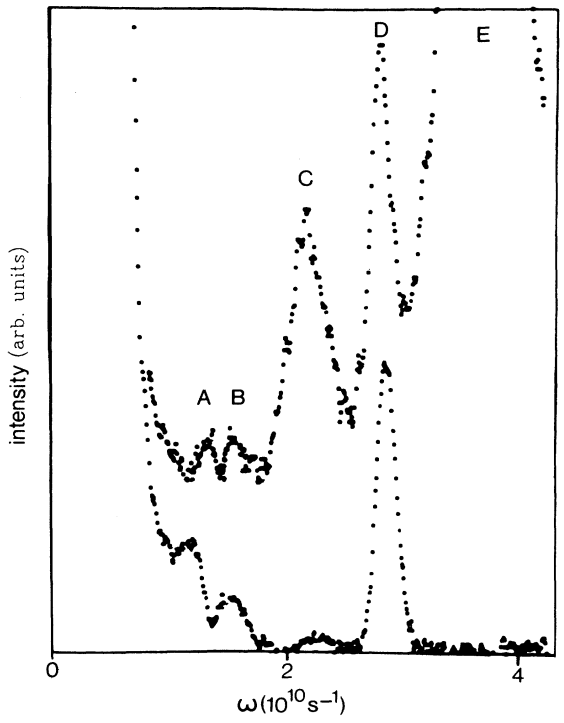

FIG. 3. Two typical spectra with scattering angles $\theta=55°$ (top) and $\theta=55°12'$ (bottom) from the interface of the quartz with the demixed binary-liquid system. *A* and *B* are scattering from the interface modes, *C* is the bulk sound mode of the cyclohexane-rich phase, *D* and *E* are quartz Brillouin lines (longitudinal mode), *D* direct, order 2, *E* totally reflected, order 2 (the order is the multiple of the free spectral range to be added to ω). The high intensity at zero frequency is due to interface imperfections. The frequency scale equals half of the free spectral range.

be used as an internal reference to calibrate frequency and wave vector. The frequencies of the remaining two peaks (A and B) are plotted against the wave vector in Fig. 4, together with the bulk sound mode. Figure 4 demonstrates the usual linear dispersion $\omega = c_s \Delta k$ for the bulk mode, where c_s is the adiabatic sound velocity. A least-squares fit to the data yields the adiabatic sound velocity of the cyclohexane-rich phase; $c_s = 1204 \pm 8$ m s^{-1}, in agreement with the literature value [21]: $c_s = 1210$ m s^{-1}. The frequencies of the other two modes appear below this line, obviously not on straight lines through the origin. Returning to the original spectra, we see that if the cell is turned through 0.20°—hereby diminishing the penetration depth of the evanescent wave from 1.2 to 0.8 μm while leaving the scattering geometry practically unaltered—the amplitude of the bulk sound mode decreases dramatically, whereas the intensity of the two peaks that we now identify as interface modes gains about a factor of 2 in magnitude. Moreover, fluctuating hydrodynamics [4] predict that, when neglecting possible mode-coupling effects, the dispersion of interface modes is linear in the component of the wave vector parallel to the interface, $\omega \sim \Delta k_{\parallel}$, and should be independent of the normal component of the wave vector, $\Delta k_{\perp}$. Plotting the frequencies as a function of $\Delta k_{\parallel}$ (Fig. 5), it appears that, indeed, the points are on two different straight lines through the origin. Thus by measurement of the dynamic structure factor $S(k,\omega)$ for different values of k we have found two interfacial fluid modes, with a linear dispersion relation that depends only on $\Delta k_{\parallel}$. Also the possibility of changing the penetration depth appreciably without changing the scattering geometry significantly is essential for the accurate measurement of the small-amplitude interfacial modes.

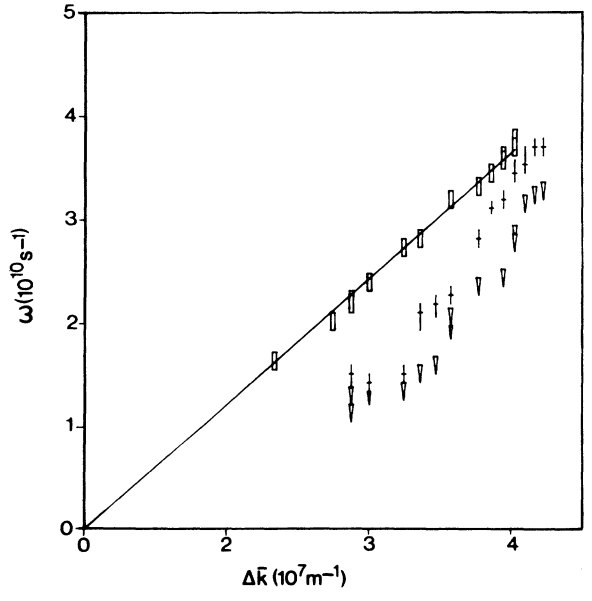

FIG. 4. Dispersion relations ω vs $\Delta k = k_f - k_i$ for the fluid and interfacial modes. Boxes: bulk mode. The straight line has a slope that equals the bulk sound velocity of the cyclohexane-rich phase, $c_s = 1204 \pm 8$ m s^{-1}. Plusses and triangles: "fast" and "slow" interface modes, respectively.

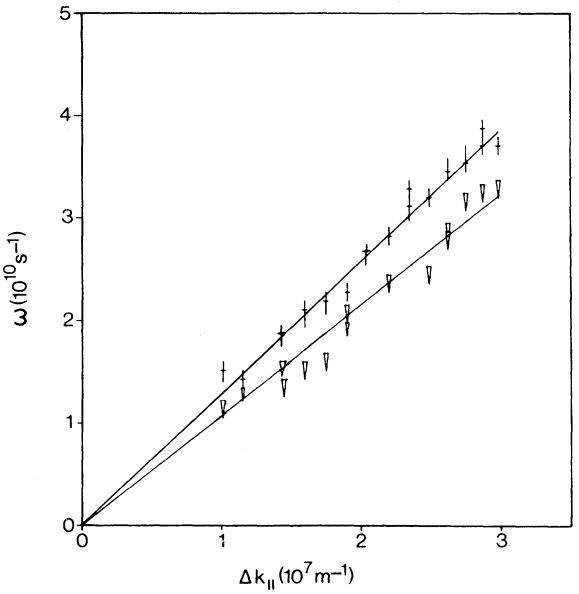

FIG. 5. Dispersion relation of the interface modes: ω vs the part of the scattering vector parallel to the interface, $\Delta k_{\parallel} = (k_i - k_f)_{\parallel}$. Plusses: fast mode. The straight line has a slope $v_B = 1301 \pm 15$ m s^{-1}. Triangles: slow mode. The line has a slope $v_A = 1078 \pm 20$ m s^{-1}.

From the dispersion relations depicted in Figs. 4 and 5, we can extract the propagation velocities $v_{A,B} = \omega_{A,B} / \Delta k_{\parallel}$ of these modes. For the slower of the two modes (peak A), we find a propagation velocity $v_A = 1078 \pm 20$ m s^{-1} whereas the methanol bulk mode propagates with a velocity $c_s = 1081 \pm 10$ m s^{-1}. Independent measurement of the bulk and the interface modes at the interface of the methanol-rich phase and the quartz [denoted as 2 in Fig. 1(a)] shows that an interfacial mode with the same dispersion relation as the "slow" mode in the wetting layer is found here. The surprising result is that, although the fast mode (peak B) seems to have the predicted linear dispersion relation, its propagation velocity $v_B = 1301 \pm 15$ m s^{-1} is significantly higher than the bulk sound velocity in either of the two fluid phases. The bulk modes of the cyclohexane-rich phase, measured in the *same* experiment, has an adiabatic sound velocity $c_s = 1204 \pm 8$ m s^{-1}. Independent measurement of the cyclohexane-quartz interface mode in another cell with only cyclohexane reveals the presence of an interface mode that has, again, the same propagation velocity as the bulk mode.

The results for the propagation velocities as a function of the wave number of the excitation (Δk for the bulk modes, $\Delta k_{\parallel}$ for the interface modes) for both the bulk fluid and the interface waves are summarized in Fig. 6. The propagation velocity of the slow mode is, within the experimental error, equal to the adiabatic sound velocity of the methanol-rich phase. Also, it can be observed that, within the experimental resolution, there is a clear

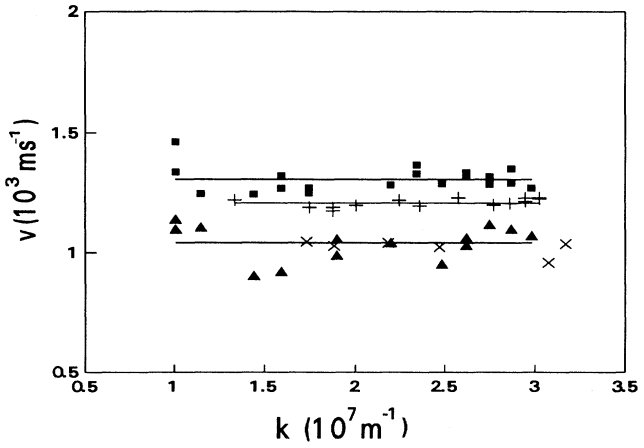

FIG. 6. Propagation velocities of the bulk and interface modes vs the wave number of the excitations, Δk for bulk modes, $\Delta k_{\|}$ for the interface modes. Lowest line: slow interface mode measured in the wetting layer (triangles) and bulk methanol sound mode measured at the quartz-bulk methanol interface (crosses), $c_s = 1081\ \mathrm{m\,s^{-1}}$. Plusses: bulk sound mode of the cyclohexane-rich phase, $c_s = 1204\ \mathrm{m\,s^{-2}}$. Boxes: propagation velocity of the fast interface modes, $v_B = 1301\ \mathrm{m\,s^{-2}}$.

distinction between the velocities of the fast interface wave and the bulk sound waves in the cyclohexane-rich phase.

To account for the damping of the waves, the peak width of both the bulk and the interface modes are plotted in Fig. 7 as a function of the squared wave number k^2 of the excitation, Δk^2 for the bulk modes and $\Delta k_{\|}^2$ for the interface modes. As can be observed from the figure, the

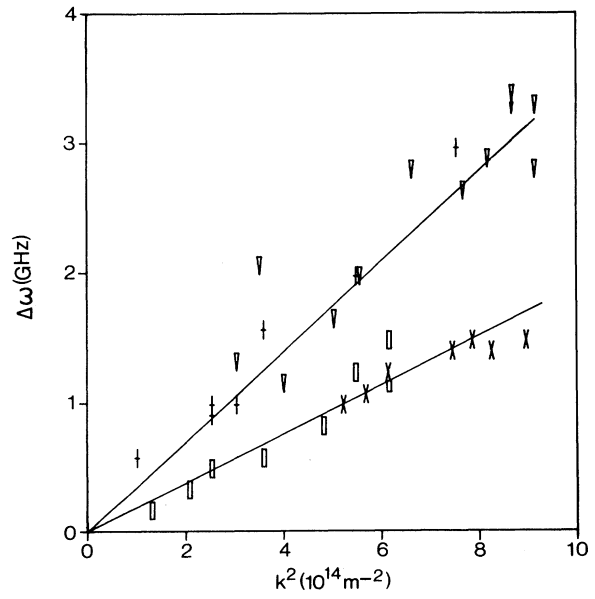

FIG. 7. Damping of the bulk and interfacial modes $\Delta\omega$ vs the squared wave number of the excitation. Triangles and plusses: cyclohexane bulk mode and fast interface mode, respectively. Squares and crosses: methanol bulk sound mode [measured at location 2 in Fig. 1(a)] and slow interface mode, respectively.

fast interface mode has the same damping as the bulk sound mode of the cyclohexane-rich phase, and the damping coefficient for the slowinterface mode is approximately the same as that for the methanol-rich phase.

Summarizing, in the presence of a wetting layer in the scattering volume, the dynamic structure factor $S(k,\omega)$ exhibits two new peaks which are interfacial fluid modes. One of these modes has a propagation velocity that equals the bulk sound velocity of the wetting phase. The other interface mode has a velocity higher than the sound velocity in either of the two liquid components. The damping of the interfacial waves depends only on the component of the wave vector parallel to the interface and is, within the experimental error, equal to the damping of the corresponding bulk sound modes.

HYDRODYNAMICS

Stimulated by these results, we performed a hydrodynamic calculation to account for the existence of the two interface modes, their propagation velocities, and their damping coefficients. For our system the acoustic impedances, the product of the density ρ and the adiabatic sound velocity c_s, are $\rho c_s = 9.3\times10^5\ \mathrm{kg\,m^{-2}\,s^{-1}}$ for the cyclohexane-rich phase and $\rho c_s = 8.4\times10^5\ \mathrm{kg\,m^{-2}\,s^{-1}}$ for the methanol-rich phase. Parameters for quartz are $\rho = 2.1\times10^3\ \mathrm{kg\,m^{-3}}$, the longitudinal sound velocity $c_l = 5730\ \mathrm{m\,s^{-1}}$, and the transversal sound velocity $c_t = 3720\ \mathrm{m\,s^{-1}}$.

In the small wave-vector limit the dynamic structure factor $S(k,k_{\|},\omega)$ close to an interface can be calculated by solving the hydrodynamic equations together with the appropriate boundary conditions [4,6]. The boundary conditions to be fulfilled are the continuity of normal and tangential stresses and the continuity of the normal displacements at the interface. For the wetting system under discussion here two interfaces are relevant: a solid-liquid and a liquid-liquid interface separated by a distance d. In Cartesian coordinates, with the z axis normal to the surface, the components of the fluctuating part of the stress tensor in an isotropic elastic solid are

$$\sigma_{szz} = \rho_s \left[c_l^2 \frac{\partial u_{sz}}{\partial z} + (c_l^2 - 2c_t^2)\phi_s \right],$$
$$\sigma_{szx_i} = \rho_s c_t^2 \left[\frac{\partial u_{sz}}{\partial x_i} + \frac{\partial u_{sx_i}}{\partial z} \right], \tag{2}$$

where $x_i = x,y$, the subscript s stands for solid, ρ is the density, c_l and c_t are the longitudinal and transversal sound velocities, u is the displacement, and $\phi = \partial u_{sx}/\partial x + \partial u_{sy}/\partial y$. For a Newtonian fluid, these components of the stress tensor are given by

$$\sigma_{zz} = -\delta p + \rho \left[\Gamma_v \frac{\partial u_z}{\partial z} + (\Gamma_v - 2\nu)\phi \right],$$
$$\sigma_{zx_i} = \rho\nu \left[\frac{\partial u_z}{\partial x_i} + \frac{\partial u_i}{\partial z} \right], \tag{3}$$

where $x_i = x,y$, u now stands for the velocity field, ν is the kinematic and Γ_v the longitudinal viscosity and δp is the

fluctuating pressure. It has been shown elsewhere that [4], together with the continuity of velocities at the interface, these equations constitute a complete set of boundary conditions on the hydrodynamic variables. After taking the appropriate Fourier and Laplace transforms these equations can be solved and yield the dispersion relations of the interface modes.

Then, limiting ourselves to first order in the wave vector k it can be shown that the dispersion relations we seek are roots of the complex eigenvalue equation:

$$[\alpha_3\gamma_2-\alpha_2\gamma_3][4(\rho_1/\rho_2)\alpha_2 k_\parallel^2(\alpha_1\beta_1+p^2)+\alpha_1 k_t^4]+[\alpha_3\gamma_2+\alpha_2\gamma_3][4(\rho_1/\rho_2)\alpha_2 k_\parallel^2(\alpha_1\beta_1+p^2)-\alpha_1 k_t^4]\exp(-2i\alpha_2 d)=0 , \tag{4}$$

where ρ_i is the density of phase i and the indices 1,2, and 3 refer to the solid phase, the methanol-rich phase, and the cyclohexane-rich phase, respectively. Here

$$\alpha_i=(\omega^2/c_i^2-k_\parallel^2)^{1/2},\quad \beta_1=(\omega^2/c_t^2-k_\parallel^2)^{1/2} ,$$
$$\gamma_i=\rho_i c_i^2(k_\parallel^2+\alpha_i^2),\quad p=(k_\parallel^2-k_t^2/2)k_\parallel^{-1} ,$$

where c_i is the longitudinal bulk sound velocity of phase i, c_t is the transverse sound velocity of the solid, and $k_t=\omega/c_t$. Numerical evaluation of the equation shows that, apart from the well-known Rayleigh wave, there are two solutions, corresponding to two interfacial fluid modes. The result is shown in Fig. 8, where the propagation velocities are shown as a function of the reduced wave vector, the product of the layer thickness d and the wave factor $k_\parallel$. The velocity of one of the modes is independent of $k_\parallel d$, $v\cong c_2$ (the sound velocity in the methanol-rich phase). The other mode has a propagation velocity that goes from $v=c_3$ (c_s in the cyclohexane-rich phase) in the limit of small reduced wave vector $k_\parallel d$ to $v=c_2$ in the limit of large $k_\parallel d$. A density-of-states calculation, equal to that presented by Jing, Sheng, and Zhou [22] for a suspension of coated colloidal particles, yields the same result [23]. Both calculations also show that if, for the fast mode, the reduced wave vector $k_\parallel d$ exceeds a cutoff given by $n2\pi$, where n is an integer, that there appear n waveguide modes with a slightly higher phase velocity.

This implies that in the limit of small reduced wave vector the velocities of the interface modes should approximately be equal to the sound velocities of the corresponding bulk modes. We believe the measurements to be in the limit of small reduced wave vector, since a sensible estimate for the layer thickness is $d\cong 300$ Å. Then $k_\parallel d$ varies between 0.3 and 0.9 in our experiments. In this limited wave-vector range there is no observable dispersion in the calculated velocities. In Fig. 9 the results of the calculation are compared with the experimental data, taking $d=300$ Å. Although there may be agreement in a qualitative sense, it is immediately clear that the measured and calculated propagation velocities for the fast mode are not in quantitative agreement. Also, no agreement can be found by taking a different layer thickness, since, by assuming that the measurement are in the limit of small $k_\parallel d$, the calculated velocity already has its highest possible value.

In deriving the equation, all higher-order effects have

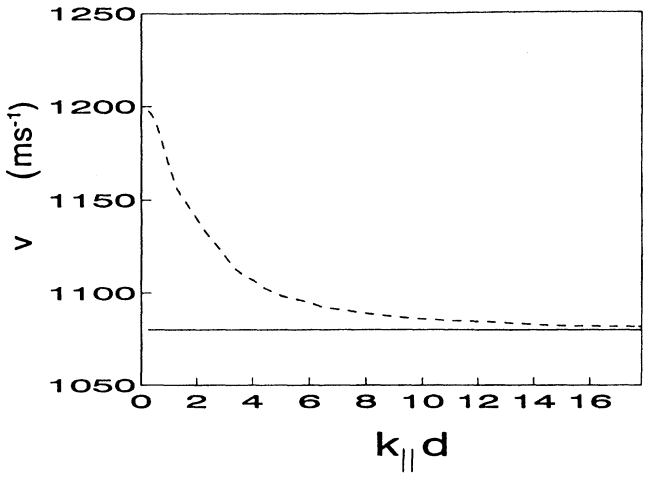

FIG. 8. Propagation velocities of the two interface modes calculated from Eq. (4). The wave vector is normalized on the layer thickness.

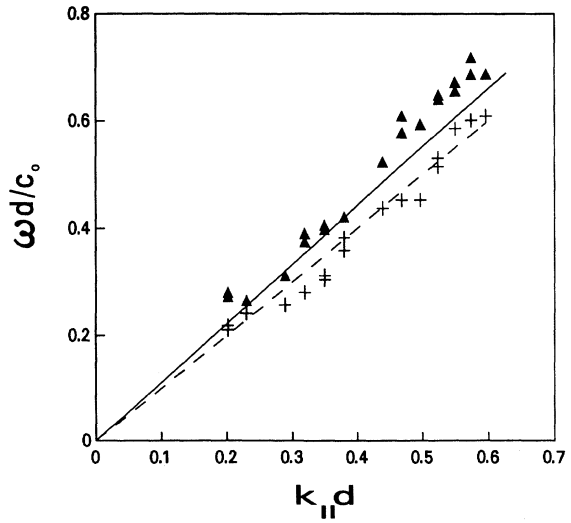

FIG. 9. Comparison between theory and experiment: the dispersion relations in dimensionless units calculated from Eq. (4) for the wetting layer thickness $d=300$ Å. The wave vector is normalized on the layer thickness, the frequency on the layer thickness and the sound velocity of the methanol-rich phase. Experimental data are shown as triangles (fast mode) and plusses (slow mode).

been neglected. This means that (i) dissipative (viscous) effects have not been taken into account. Also, (ii) the influence of interfacial energy transport has not been considered; if the sound is not isothermal, $\gamma=(C_p/C_v)\neq 1$, the propagation velocity of the interface modes can be altered due to heat conduction between the two phases depending on the ratio of thermal diffusivities of the two components. However, both the viscous and the thermal penetration depth [24], $d_\nu=(2\nu/c_s k)^{1/2}$, $d_T=(2D_T/c_s k)^{1/2}$, are estimated to be on the order of 100 Å and thus do not exceed the estimated film thickness. For the two modes that were observed experimentally, the viscous penetration depth is calculated to be 100 Å for the fast mode and 85 Å for the slow mode. This would mean that the two effects mentioned above do not have a very large influence on the propagation velocities of the interface modes. Finally, (iii) the possible coupling of the interface waves with the capillary waves has not been considered up till now; in first approximation only the capillary waves at the liquid-liquid interface would have to be taken into account, due to the high stiffness of the solid phase. The inclusion of the surface tension leads to a different boundary condition for the normal stresses at the liquid-liquid interface [25]:

$$(\sigma_{zz_2}-\sigma_{zz_3})-\tfrac{1}{2}\gamma k_\parallel^2(u_{z_2}+u_{z_3})=0\ , \tag{5}$$

where 2 and 3 again denote the methanol-rich and the cyclohexane-rich phases, the σ_{zz} terms are given by Eq. (3), and γ is the interfacial tension of the liquid-liquid interface. Together with the boundary condition for the velocities the inclusion of the surface tension term produces a new solution at low frequencies (and large layer thickness) of Eq. (4):

$$\omega=\left[\frac{\gamma}{\rho_2+\rho_3}\right]^{1/2}k_\parallel^{3/2}\ , \tag{6}$$

which is the well-known dispersion relation of capillary waves at a fluid-fluid interface [26]. However, the inclusion of this term in the boundary condition produces a very small effect on the propagation velocities of the interface modes. ALso, the inclusion of either the thermal diffusivity and/or the viscosity does not cause a significant shift in the calculated propagation velocities. Numerical evaluation of Eq. (4) with the inclusion of these terms confirms this. Thus the remaining discrepancy between theory and experiment may not be resolved by including higher-order effects in the calculation.

To summarize, in the hydrodynamic calculation, the adiabatic compressibility $\chi_s=1/(\rho c_s^2)$, which gives the propagation velocities of the sound and interface waves, it taken to be the same for both the bulk and the interface. In the limit of small $k_\parallel d$ the calculation predicts that the interface modes should have the same velocity as the corresponding bulk modes. The measurements, however, indicate that the local compressibility at the interface, which determinates the propagation velocity of the fast interface mode, is different from that in the bulk. It is therefore proposed that the observed velocity shift is caused by the viscoelasticity of the interface, which amounts to the introduction of a local "surface" compressibility that can, in general, be different from its bulk value.

VISCOELASTICITY

The viscoelastic regime, intermediate between the low-frequency hydrodynamic and high-frequency elastic behavior, can be described [27] phenomenologically by the introduction of frequency-dependent elastic moduli and a frequency-dependent viscosity $\eta(\omega)$. The viscosity is then given by

$$\eta(\omega)=\frac{G_\infty\tau}{(1+i\omega\tau)}\ , \tag{7}$$

where G_∞ is the high-frequency shear modulus and τ is the stress relaxation time of the system, also referred to as the Maxwell relaxation time. The frequency dependence of the shear modulus G and the bulk modulus K is then given by

$$\begin{aligned} G(\omega)&=i\omega\eta(\omega)\ ,\\ K(\omega)&=K_0+i\omega\eta(\omega)\ , \end{aligned} \tag{8}$$

where K_0 is the reciprocal adiabatic compressiblity. Then the behavior of the fluid crosses over from viscous at low frequencies to elastic at high frequencies. The velocity c_l of the longitudinal waves traveling in the viscoelastic medium is determined by the elastic constant c_{11} and is given by [7]

$$c_l=\left[\frac{c_{11}}{\rho}\right]^{1/2}\ , \tag{9}$$

where ρ is the mass density and c_{11} can be written in terms of the bulk and shear moduli as $c_{11}=(K+\frac{4}{3}G)$. In analogy to the treatment for bulk phases, Tejero and Baus [7] have shown that the viscoelastic equations for a surface can be obtained by introducing surface Maxwell formulas equal to those presented above, but with the relevant quantities (elastic constants and viscosities) replaced by their surface excess values [28]. The propagation velocities of the longitudinal interfacial waves is now determined by the *surface elastic constant* $\bar{c}_{11}$. Taking the measured value $c_l=1301\ \mathrm{m\,s^{-1}}$, this yields $\bar{c}_{11}=1.3\times10^9\ \mathrm{N/m^2}$, about 15% higher than the measured bulk value for the cyclohexane-rich phase.

A rough estimate of the relaxation time can be obtained from the approximate relation [27]

$$\tau^{-1}=\frac{2}{\sqrt{\pi}}\left[\omega_1^2-\frac{\omega_0^2}{S(k)}\right]\ , \tag{10}$$

where ω_1 is the measured frequency, ω_0 the frequency in the thermodynamic limit, and $S(k)$ the static structure factor. If the structure factor at these large scales is taken as unity, one finds a relaxation time $\tau=9\times10^{-11}$ s, a very slow relaxation time, since for normal (molecular) bulk liquids, τ is on the order of 10^{-12} s.

In principle, since τ is the only parameter in this model, it would now be possible to calculate the elastic moduli $\bar{K}$ and $\bar{G}$ and thus the viscoelastic response over the en-

tire frequency regime. However, since these measurements are in a very limited wave vector range, $10^7 < k_{\parallel} < 3\times 10^7$, and thus effectively represent only a single frequency point in the entire viscoelastic regime, this does not seem justifiable and will not be pursued here. Also, it should be noted that, in general, one would expect a viscoelastic wave to have a smaller damping than the corresponding hydrodynamic wave. In our case, however, the errors in the measured attenuation coefficients are too large to draw any rigorous conclusions about a possible change in the damping of the waves. From Fig. 7 it may be concluded that, if such an effect is observed, it is in any case a change of less than 50%.

DISCUSSION

Brillouin scattering from an evanescent wave has been used to study the equilibrium fluctuations in a system with a wetting layer that intrudes between a fluid and a solid wall. In this way, two fluid interfacial modes were found, one of which has a propagation velocity equal to the sound velocity in the wetting phase. The other interfacial mode has a propagation velocity higher than that of the corresponding bulk mode. In the normal hydrodynamic description, the exchange of energy and momentum across the interface can alter both the linear dispersion relation and the propagation velocity of the interface waves. For our system, however, it can be shown that these effects are negligible and thus cannot explain the alteration of the velocity. This leads us to the inference that the bulk transport properties are not the same as those governing the surface dynamics. The transport properties can then be described by the introduction of surface elastic moduli. As there is no *a priori* knowledge of the magnitude of these quantities, they have to be determined experimentally. Our measurements give an indication for the value of $\bar{c}_{11}$, but span only a very limited wave-vector range. It would therefore be very interesting to repeat the experiments over a much larger range, which would allow for a rigorous comparison with the predictions of viscoelastic theory. The interest of such a comparison lies in the fact that the elastic moduli can be written in terms of the pair distribution function [27] $g(r)$ and thus provide information on the *structure* of the fluid interface, a still-standing problem in statistical mechanics.

ACKNOWLEDGMENTS

This work is part of the research program of the Foundation for Fundamental Research of Matter (FOM) and was made possible by financial support from the Netherlands Organization for Scientific Research (NWO). We would like to thank Dr. P. Sheng for helpful correspondence.

[1] R. Loudon, in *Surface Excitations,* edited by V. M. Agranovich and R. Loudon (North-Holland, Amsterdam, 1984).
[2] J. G. Dil, Rep. Prog. Phys. **45**, 285 (1982).
[3] J. C. Earnshaw, in *Fluid Interfacial Phenomena,* edited by C. A. Croxton (Wiley, New York, 1986).
[4] D. Gutkowicz-Krusin and I. Procaccia, Phys. Rev. Lett. **48**, 417 (1982); Phys. Rev. A **27**, 2585 (1983); D. Gutkowicz-Krusin, *ibid.* **28**, 1602 (1983).
[5] S. Goldstein, *Modern Developments in Fluid Dynamics* (Clarendon, Oxford, 1938) (reprinted by Dover, New York, 1965), pp. 676–680.
[6] L. M. Brekhovskikh, *Waves in Layered Media* (Academic, New York, 1980); W. M. Ewing, W. S. Jardetzky, and F. Press, *Elastic Waves in Layered Media* (McGraw-Hill, New York, 1957).
[7] C. F. Tejero and M. Baus, Mol. Phys. **54**, 1307 (1985); C. F. Tejero, M. J. Rodriguez, and M. Baus, Phys. Rev. A **29**, 2179 (1984); M. Baus and C. F. Tejero, J. Chem. Phys. **78**, 483 (1983).
[8] D. Bedeaux, A. M. Albano, and P. Mazur, Physica A **82**, 438 (1976); D. Bedeaux and I. Oppenheimer, *ibid.* **90**, 487 (1978).
[9] B. U. Felderhof, Physica **48**, 541 (1970).
[10] F. C. Goodrich, Proc. R. Soc. London, Ser. A **374**, 341 (1981).
[11] M. A. Bouchiat and J. Meunier, J. Phys. (Paris) **32**, 561 (1971); D. Langevin and J. Meunier, J. Phys. (Paris) Colloq. **44**, C3-10 (1983).
[12] D. Byrne and J. C. Earnshaw, J. Phys. D **12**, 1133 (1979).
[13] E. F. Gramsbergen, A. H. Stiphout, and G. H. Wegdam, Phys. Rev. A **40**, 5437 (1989).
[14] J. G. Dil and E. M. Brody, Phys. Rev. B **14**, 5218 (1976).
[15] M. R. Moldover and J. W. Cahn, Science **207**, 1075 (1980).
[16] P. G. deGennes, Rev. Mod. Phys. **57**, 827 (1985).
[17] O'D. Kwon, D. Beaglehole, W. W. Webb, B. Widom, J. W. Schmidt, J. W. Cahn, M. R. Moldover, and B. Stephenson, Phys. Rev. Lett. **48**, 185 (1982); D. Beaglehole, J. Phys. Chem. **87**, 4749 (1983); D. Bonn, H. Kellay, and G. H. Wegdam, Phys. Rev. Lett. **69**, 1975 (1992).
[18] K. H. Lan, N. Ostrowski, and D. Sornette, Phys. Rev. Lett. **57**, 17 (1986).
[19] M. Born and E. Wolf, *Principles of Optics* (Pergamon, Oxford, 1964).
[20] B. Berne and R. Pecora, *Dynamic Light Scattering* (Wiley, New York, 1976).
[21] *Molecular Acoustics,* Landolt-Börnstein, New Series, Group 2, Vol. 5 (Springer-Verlag, Berlin, 1967).
[22] X. Jing, P. Sheng, and M. Zhou, Phys. Rev. Lett. **66**, 1240 (1991); Phys. Rev. A **46**, 6513 (1992).
[23] Ping Sheng (private communication).
[24] J. C. Nieuwoudt, T. R. Kirkpatrick, and J. R. Dorfman, J. Stat. Phys. **34**, 203 (1984).
[25] J. Joosten, in *Thin Liquid Films,* edited by B. I. Ivanov (Marcel Dekker, New York, 1988).
[26] V. G. Levich, *Physico-Chemical Hydrodynamics* (Prentice-Hall, Englewood Cliffs, NJ, 1962).
[27] J. P. Boon and S. Yip, *Molecular Hydrodynamics* (McGraw-Hill, New York, 1980); J. P. Hansen and I. R. McDonald, *Theory of Simple Liquids* (Academic, London, 1976).
[28] Note, however, that for an interface $c_{44} \neq c_{66}$, see p. 1315 of C. F. Tejero and M. Baus, Mol. Phys. **54**, 1307 (1985).